Article

Current Biology

Abnormal Locus Coeruleus Sleep Activity Alters Sleep Signatures of Memory Consolidation and Impairs Place Cell Stability and Spatial Memory

Highlights

- Locus coeruleus (LC) spikes coincide with the waning phase of sleep spindles
- LC activity during sleep interferes with NREM delta, sleep spindles, and REM theta
- Sleep with abnormal LC activity hampers next day CA1 spatial mapping
- Normal LC silences during sleep are necessary for proper memory consolidation

Authors

Kevin M. Swift, Brooks A. Gross, Michelle A. Frazer, ..., Anthony E. Pickering, Susan J. Sara, Gina R. Poe

Correspondence

ginapoe@ucla.edu

In Brief

Swift et al. show that overactivity of the locus coeruleus, the main source of norepinephrine to the forebrain, during sleep interferes with signatures of NREM sleep and REM sleep associated with sleep-dependent memory consolidation. Maladaptive LC activity can impair next day hippocampal spatial encoding, producing long-term behavioral deficits.

Swift et al., 2018, Current Biology *28*, 3599–3609
November 19, 2018 Crown Copyright © 2018 Published by Elsevier Ltd.
https://doi.org/10.1016/j.cub.2018.09.054

CellPress

Current Biology
Article

Abnormal Locus Coeruleus Sleep Activity Alters Sleep Signatures of Memory Consolidation and Impairs Place Cell Stability and Spatial Memory

Kevin M. Swift,[1] Brooks A. Gross,[2] Michelle A. Frazer,[2] David S. Bauer,[1] Kyle J.D. Clark,[1] Elena M. Vazey,[3] Gary Aston-Jones,[4] Yong Li,[5] Anthony E. Pickering,[5] Susan J. Sara,[6,7] and Gina R. Poe[2,8,*]
[1]Department of Molecular and Integrative Physiology, University of Michigan, Ann Arbor, MI 48109, USA
[2]Integrative Biology and Physiology Department and Department of Psychiatry and Biobehavioral Sciences, University of California, Los Angeles, Los Angeles, CA 90095, USA
[3]Department of Biology, University of Massachusetts, Amherst, MA 01003, USA
[4]Brain Health Institute, Rutgers University, New Brunswick, NJ 08854, USA
[5]School of Physiology, Pharmacology & Neuroscience, University of Bristol, Bristol BS8 1TD, UK
[6]Center for Interdisciplinary Research in Biology, College de France, Paris 75005, France
[7]Child and Adolescent Psychiatry, New York University Medical School, New York, NY 10003, USA
[8]Lead Contact
*Correspondence: ginapoe@ucla.edu
https://doi.org/10.1016/j.cub.2018.09.054

SUMMARY

Sleep is critical for proper memory consolidation. The locus coeruleus (LC) releases norepinephrine throughout the brain except when the LC falls silent throughout rapid eye movement (REM) sleep and prior to each non-REM (NREM) sleep spindle. We hypothesize that these transient LC silences allow the synaptic plasticity that is necessary to incorporate new information into pre-existing memory circuits. We found that spontaneous LC activity within sleep spindles triggers a decrease in spindle power. By optogenetically stimulating norepinephrine-containing LC neurons at 2 Hz during sleep, we reduced sleep spindle occurrence, as well as NREM delta power and REM theta power, without causing arousals or changing sleep amounts. Stimulating the LC during sleep following a hippocampus-dependent food location learning task interfered with consolidation of newly learned locations and reconsolidation of previous locations, disrupting next-day place cell activity. The LC stimulation-induced reduction in NREM sleep spindles, delta, and REM theta and reduced ripple-spindle coupling all correlated with decreased hippocampus-dependent performance on the task. Thus, periods of LC silence during sleep following learning are essential for normal spindle generation, delta and theta power, and consolidation of spatial memories.

INTRODUCTION

Much work has focused on the interplay between the hippocampus and neocortex during sleep to promote memory [1–4]. However, the neuromodulatory systems necessary for memory formation during waking are relatively unexamined during sleep. The noradrenergic system and its source for the forebrain, the locus coeruleus (LC), is active during waking to promote vigilance and is responsive to novel information, enabling rapid learning by boosting long-term potentiation (LTP) mechanisms [5, 6]. During sleep, decreased LC neuronal activity was thought to simply promote somnolence [7].

The decrease in LC firing is not uniform across all phases of sleep in rats and higher mammals [8–10]. The LC is active throughout the slow wave sleep stage of non-REM (NREM) sleep, but LC neurons fall silent prior to the onset of each sleep spindle (10- to 15-Hz high-amplitude, 0.3-3 s long oscillations in electrographic signals) in NREM sleep [10]. During rapid eye movement (REM) sleep, LC neurons also fall silent while cholinergic activity increases [10] and 5-9 Hz theta frequency activity dominates in the electrographic signals. Both REM sleep theta and sleep spindles have been shown to be important for memory consolidation [11–14], but the physiological relevance of these LC silences for the function of sleep for memory has not been evaluated. We hypothesize that, because norepinephrine supports strengthening of neuronal synapses (LTP) in memory circuits, these transient LC silences uniquely allow depotentiation (resetting strengthened synapses to baseline efficacy) that is necessary for certain types of learning [15, 16].

We tested whether normal transient decreases in LC firing are necessary for the generation of normal REM sleep theta and NREM sleep spindles as well as for memory consolidation and next day memory neural encoding. Using optogenetics to maintain waking LC activity levels during NREM and REM sleep combined with simultaneous tetrode recordings of hippocampal place cells during place learning, we tested the effect of increased LC activity during sleep on a sleep-dependent hippocampal place memory learning task [17]. Although the stability and duration of sleep states were not changed, the learning-related signatures of NREM and REM sleep were impaired. Results showed that LC silences are necessary for normal NREM sleep delta power, REM sleep theta power, sleep spindle generation, and the coupling of sleep spindles to hippocampal

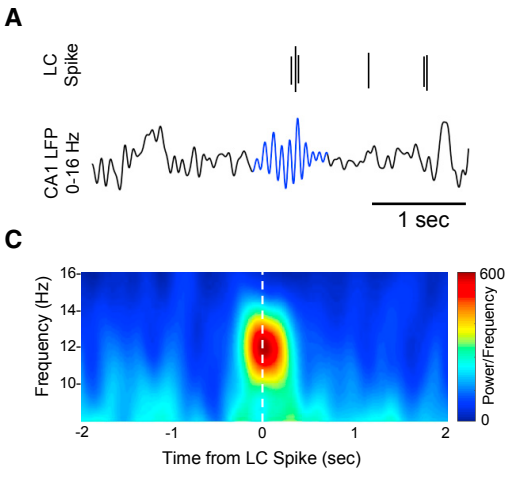

Figure 1. LC Spikes Synchronize to Peak Spindle Power, and LC Optogenetic Stimulation Decreases Spindle Occurrence

(A) Example of LC spike timing in relation to spindles. LC activity ceases prior to spindle onset, and during the spindle (in blue) LC activity returns, leading to a decrease in spindle power.

(B) Normalized root-mean-square of spindle power (10–15 Hz) during sleep spindles centered on LC spikes. The blue line represents the mean (± SEM) effect of LC spikes on spindle power when spikes occur within identified spindles, whereas the dark gray line represents the effect of LC spikes on mean spindle power (± SEM) outside of identified spindles (n = 3 rats). The light gray area indicates values with significant differences between the two with significance from $p < 0.05$ to $p < 0.0001$ from $t = -0.67$ to $t = 0.54$ s.

(C) Example heatmap displaying rise and fall of spindle power (color bar in μV^2/Hz) centered on LC spikes occurring within the spindles (n = 561 spindles from three animals).

(D) Two-hertz LC stimulation during sleep decreases CA1 spindle occurrence rate in ChR2+ rats, n = 4. Paired t test ***p = 0.0003. Data are displayed as mean ± SEM.

See also Figures S1 and S2.

ripples—drops in all of which correlated with decreases in different facets of task performance. Furthermore, although overall place cell firing rates were unchanged during sleep or wakefulness, sustained LC activity during sleep also led to decreased next day encoding stability of maze locations during the task.

RESULTS

Endogenous LC Activity Decreases during Spindle-Rich Intermediate Sleep

Tetrode recording of endogenous LC neural activity across sleep and wakefulness showed highest LC activity during waking and significant reductions in activity during all stages of sleep: NREM-slow wave sleep; NREM-intermediate sleep; and REM sleep (Figure S1). Within NREM sleep, LC neuron activity during spindle-rich intermediate sleep (IS) [18] was similar to REM sleep, when LC activity reached its lowest point. Thus, both REM sleep and spindle-rich IS are periods of greatly reduced LC neuronal activity.

Endogenous LC Activity during Sleep Spindles Terminates the Spindle

Aston-Jones and Bloom [10] demonstrated that LC neurons fire with a specific temporal relationship to sleep spindles, falling silent one second prior to the onset of each sleep spindle. In the latter half of the sleep spindle, LC neurons resume firing (see example in Figure 1A). We posit that this resumption of LC activity mid-spindle leads to spindle termination, possibly through the depolarizing action of norepinephrine on thalamocortical neurons; norepinephrine repolarizes thalamocortical neuronal membranes and terminates the voltage-gated Ca^{2+} spikes that generate sleep spindles [19, 20]. We found that LC spikes within sleep spindles occurred when the spindles reached maximal power in the 10-15 Hz sigma band. These within-spindle LC spikes were followed by an immediate and rapid reduction of sigma power (Figures 1B and 1C), which supports the idea that LC activity leads to spindle termination. This phenomenon was spindle specific as LC spikes occurring outside of sleep spindles (during NREM sleep) had no effect on sigma power.

LC Optogenetic Stimulation during Sleep Decreased NREM Sleep Spindle Occurrence

Given the precise timing of LC neuronal spikes during spindles, along with previous work showing that norepinephrine infusions into thalamic nuclei *in vitro* abolishes spindle generation [20], we hypothesized that optogenetically enhanced LC activity during sleep could be used to reduce spindle occurrence during NREM sleep. To test this, we expressed channelrhodopsin (ChR2) in LC cells under the control of PRSx8, a synthetic dopamine-beta hydroxylase promoter [21] (Figure S2A). Extracellular recordings of ChR2-expressing LC cells *in vivo* showed light-evoked action potentials in response to 473-nm light pulses (Figure S2B).

We conducted a series of experiments to determine what frequency of LC stimulation was permissible to maintain sleep without evoking arousals (see STAR Methods and Figures S2C–S2E). We found 2-Hz LC stimulation did not generate arousals and, further, was within the normal physiological activity range. Therefore, 2 Hz stimulation rate was used throughout the remainder of the studies.

As predicted, stimulating noradrenergic LC neurons of ChR2+ rats at 2 Hz during sleep resulted in a significant decrease in NREM sleep spindle occurrence compared to baseline sleep lacking stimulation in the same animals (Figure 1D).

LC Stimulation during Sleep Impaired Subsequent Hippocampal Spatial Encoding

Sleep spindles are strongly implicated in memory consolidation and in the integration of new information into existing knowledge [13, 22]. Previous work from our lab showed that pharmacologically enhancing noradrenergic activity across the post-training sleep period (using the selective noradrenergic reuptake inhibitor desipramine) impaired hippocampal learning [17]. We tested

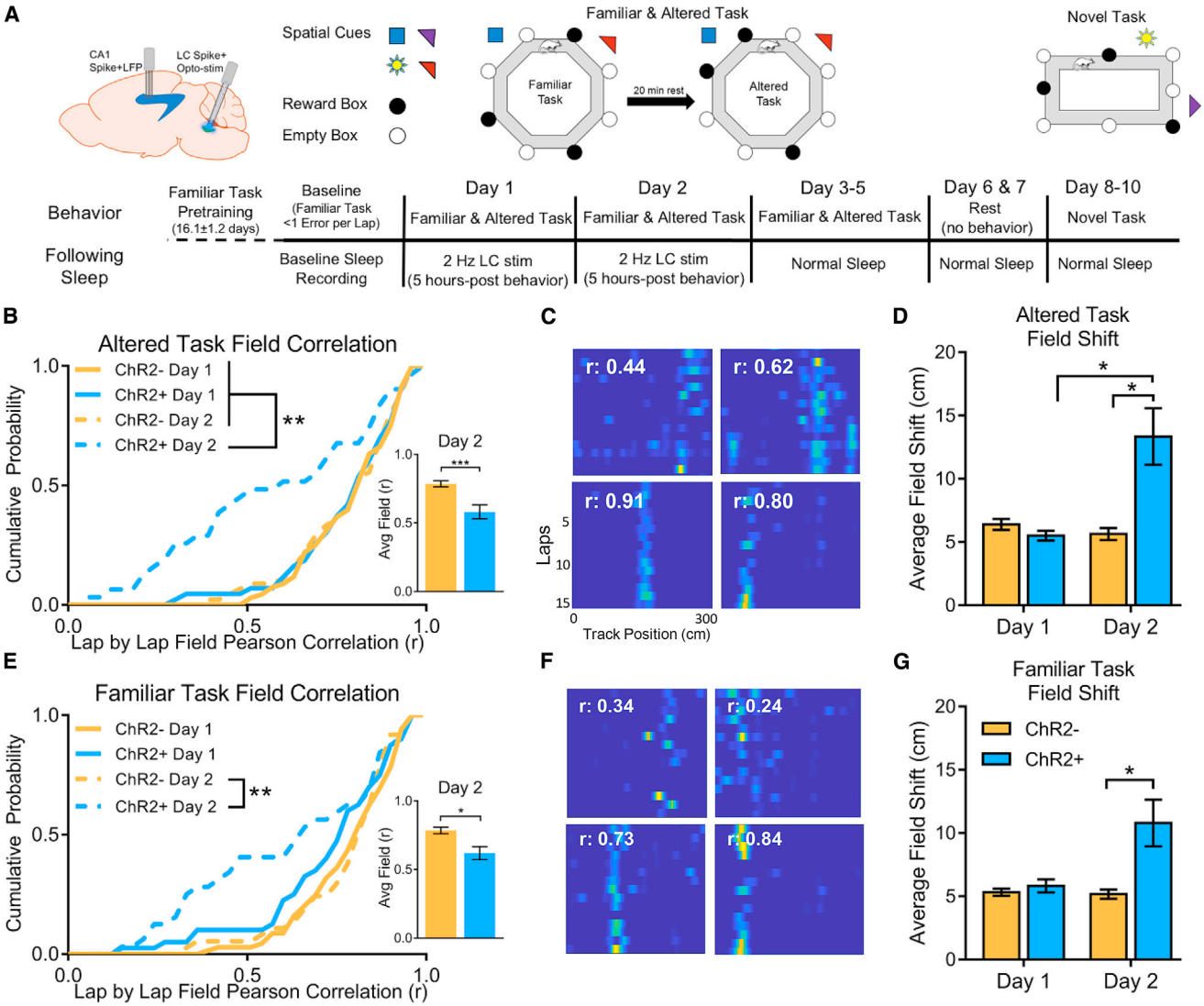

Figure 2. LC Stimulation during Sleep Impairs Next Day Place Field Encoding

(A) Illustrations of recording electrode placements in the rat brain, task layout, and experimental timeline.

(B) The cumulative probability of the lap-to-lap place field Pearson correlation on altered task. Fields with high spatial stability have a higher correlation. On day 2 ChR2+ rats show a shift toward more fields having lower correlation values. Kolmogorov-Smirnov test; **$p < 0.01$. Subplot bar graph displays the overall average day 2 field correlation. Mann-Whitney; ***$p = 0.003$.

(C) Representative heatmaps of place field spatial encoding with warmer colors displaying where CA1 pyramidal spikes were firing faster (relative to the cell's own peak rate) along the track (horizontally) and where firing occurred across multiple laps (vertically). The top two represent lower correlation fields from ChR2+ day 2. The bottom two represent higher correlation fields from ChR2− day 2.

(D) Average place field shift per lap on the altered task on day 1 and day 2. As shifts can be in positive or negative direction, the absolute value of the shifts are used to calculate the averages in (B) and (D). (B and D) ChR2− day 1 n = 61, ChR2+ day 1 n = 43, ChR2− day 2 n = 45, and ChR2+ day 2 n = 31 (outlier removed from control day 1 and control day 2). Kruskal-Wallis; Dunn post hoc: ChR2+ day 1 versus ChR2+ day 2 $p = 0.040$; ChR2− day 2 versus ChR2+ day 2 $p = 0.013$.

(E) The average lap-to-lap place field correlation on familiar task with ChR2+ day 2 rats showing decreased field correlation. Kolmogorov-Smirnov test; **$p < 0.01$. Subplot bar graph displays the overall average day 2 field correlation. Mann-Whitney; *$p = 0.023$.

(F) Representative heatmaps of place field spatial encoding on the familiar task. Top two represent lower correlation fields from ChR2+ day 2. Bottom two represent higher correlation fields from ChR2- day 2.

(G) Average place field shift per lap on the familiar task on day 1 and day 2. (E and G) ChR2 day 1 n = 66, ChR2+day 1 n = 40, ChR2 day 2 n = 37, and ChR2+ n = 32 (one outlier removed from ChR2+ day 2). Kruskal-Wallis; Dunn post hoc: ChR2− day 2 versus ChR2+ day 2 *$p = 0.046$. Bar graphs are displayed as mean ± SEM. See also Figure S3.

whether enhancing noradrenergic activity selectively during only post-training sleep was sufficient to impair hippocampal spatial encoding. Rats in a separate cohort from those shown in Figure 1 were pretrained on a hippocampus-dependent spatial learning task [23] that presented food rewards at three familiar positions on an elevated octagonal track (Figure 2A). Once the rats

reached behavioral criteria (<1 error per lap) during the training period, they ran the track daily with food at the familiar task locations and then ran the track for an additional 15 laps with two of the three food reward locations shifted to altered positions (the altered task) that remained in the same altered place for the last 15 laps each day. The function of the task was to evaluate whether rats could remember both reward location maps: the three previously consolidated familiar locations and the new altered locations. Following the familiar and altered track running sessions, we monitored rats' sleep-wake behavior via neck electromyography (EMG) and CA1 local field potential (LFP) activity and optogenetically stimulated the LC at 2 Hz whenever the rat was asleep (both NREM and REM) in the 5-hr post-learning period. This 5-hr post-learning window has been shown to be a critical period for hippocampal sleep-dependent memory consolidation (see, for review, [24]). Stimulation occurred on the first two days as, by day 3, REM sleep signs of successful memory consolidation are already apparent [25, 26].

We first examined the effect of LC stimulation on hippocampal place cell spatial encoding. Stimulating the LC during sleep after day 1 exposure to both the familiar and altered tasks resulted in reduced lap-to-lap spatial stability of place fields during both familiar and altered tasks on day 2 in ChR2+ rats (Figures 2B and 2E). Figures 2C and 2F show representative heatmaps of place field locations across laps with each field's associated stability metric (i.e., the Pearson correlation of the field firing maps across laps—higher r values represent higher spatial stability). The decrease in place field stability in ChR2+ rats went hand-in-hand with a significant increase in lap-to-lap shifts in place field location on both tasks (Figures 2D and 2G).

Next, we examined place field expansion. While performing a lap-based task, the center of mass (COM) of a place field (i.e., the region within the place field where the place cell has the highest activity) shows a net shift backward across multiple laps, expanding the overall field size as the place cell begins to fire slightly earlier on the track. This phenomenon is better known as place field backward expansion [27, 28]. Place field backward expansion is an NMDA-dependent plasticity effect [29]. As place fields do not grow across days [30] and remain relatively stable in position, the field size and center of mass must reset between days and running sessions. We have previously posited that this reset function is accomplished by depotentiation that is allowed by the absence of LC activity during REM sleep [25, 26]. The abnormal presence of LC activity during REM sleep would prevent this resetting of place field size and center of mass. We found that while place field backward expansion occurred normally on day 1 (before intervention) on both tasks, on day 2 in ChR2+ rats, the familiar place fields did not again expand backward during the maze session, but rather shifted abnormally forward (Figure S3B). There was also a significant increase in familiar task place field size on day 2 selectively in ChR2+ rats (Figure S3D). These abnormal expansion and forward shifts were not seen on the altered task (Figures S3A and S3C), suggesting a specific effect on previously consolidated, familiar spatial information.

Both spatial mapping abnormalities of place field stability and abnormal place field backward expansion indicates that LC stimulation during sleep following learning on day 1 caused abnormal CA1 place field consolidation of the altered task and abnormal reconsolidation of the familiar task. Interestingly, these effects occurred independent of any changes in CA1 pyramidal cell firing rate during NREM, REM sleep, or waking (two-way ANOVA; Sidak post hoc; $p = 0.92$, 0.66, and 0.98, respectively).

LC Stimulation during Post-Learning Sleep Impaired Spatial Learning and Memory Performance

Just as place encoding was impaired on both the altered and familiar task by enhanced LC activity during sleep, behavioral performance was similarly impaired on both tasks. On the altered task, ChR2+ rats showed no day-to-day improvement, whereas ChR2− rats improved significantly from day 1 to day 5 and performed significantly better than ChR2+ rats on day 4 and 5 (Figure 3A). Not surprisingly, given the place field encoding deficits, ChR2+ rats also performed significantly worse on the familiar task than ChR2− rats, showing a significant decline in performance between days 1 and 5, and performed worse than controls by days 4 and 5 (Figure 3B). To ensure that LC stimulation during sleep had no lasting effect on learning once the stimulation protocol ceased, the following week both groups were run on a completely novel hippocampal task with new novel spatial cues and reward locations, followed by normal sleep each day. Both groups learned the novel task at similar rates and showed significant improvement in performance within two days (Figure 3C).

LC Stimulation during Sleep Altered Task-Solving Strategies

In addition to the error count, we were curious to see whether rats utilized hippocampal strategies to solve the task or instead reverted to a random search strategy [31]. We termed errors "map errors" if they were errors committed at the reward locations that differed between the tasks and "procedural errors" if the error was at a location where the reward contingency remained static (i.e., checking any of the three box positions that were not rewarded on either the familiar or altered tasks, or skipping the one box position that was rewarded on both maze; Figure 4A). For the altered task, as expected, ChR2− rats consistently committed significantly more map errors than procedural errors, checking for food in previously rewarded positions (Figure 4B). In contrast, in LC-stimulated ChR2+ rats there was no difference in the number of map errors compared to procedural errors by day 2, and each day the average number of procedural errors climbed until they were on par with the number of map errors (Figure 4C)—suggesting adoption of a random search strategy. On the familiar task (day 1 occurred before the first exposure to the altered maze, so no familiar task map errors were possible on day 1), ChR2− rats committed significantly fewer procedural errors than map errors and showed an overall downward trend in procedural errors across days, whereas ChR2+ rats committed a similar number of procedural and map errors across days with an overall trend to increasing errors of both types across days (Figures 4D and 4E).

LC Stimulation during Sleep Altered Specific Frequency Bands, but Not Sleep Architecture

We next examined whether LC sleep stimulation caused any change in sleep characteristics. Looking first at waking, there

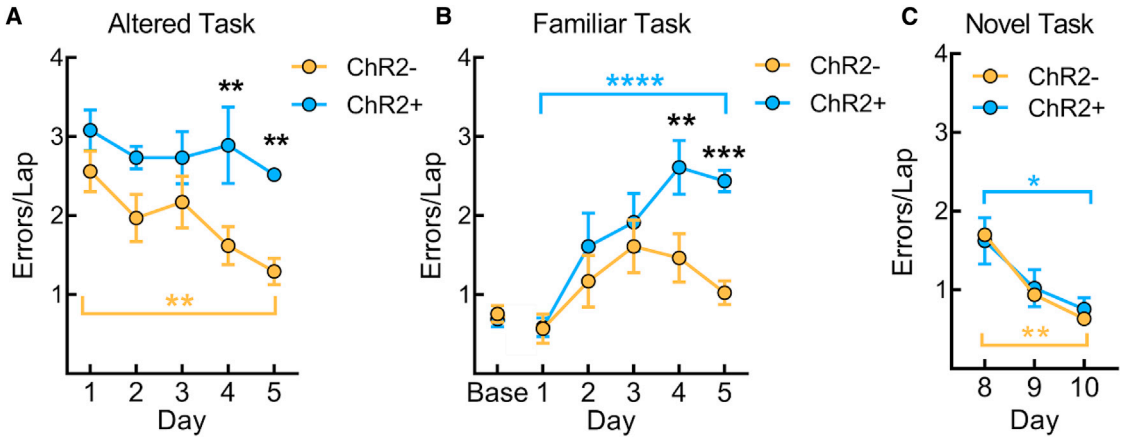

Figure 3. LC Stimulation during Sleep Impairs Learning and Memory

(A) The average errors per lap by day for the ChR2− and the ChR2+ groups on the altered task. Two-way ANOVA; Sidak post hoc (in black): ChR2− versus ChR2+ day 4 p = 0.0012; day 5 p = 0.0017. Two-way ANOVA; Tukey post hoc (in yellow): ChR2− day 1 versus day 5 p = 0.002. **p < 0.005.

(B) The average errors per lap for ChR2− and stimulated ChR2+ groups on the familiar task. Two-way ANOVA; Sidak post hoc (in black): ChR2− versus ChR2+ day 4 **p = 0.0032; day 5 ***p = 0.0004. Two-way ANOVA; Tukey post hoc (in blue): ChR2+ day 1 versus day 5 ****p < 0.0001.

(C) The average errors per lap for ChR2− and ChR2+ groups on the novel task with both groups meeting criteria of less than one error per lap after three days of maze running. Two-way ANOVA; Tukey post hoc: ChR2− day 8 versus day 10 (in yellow) **p = 0.0019; ChR2+ day 8 versus day 10 (in blue) p = 0.0084. Five rats for each group for (A) and (B) are shown; three rats for each group in (C) are shown.

Data are displayed as mean ± SEM. *p < 0.05; **p < 0.005; ***p < 0.0005; ****p < 0.0001.

was no difference in the percent of the total time spent awake between ChR2− and ChR2+ rats, i.e., LC stimulation did not prevent sleep (Figure 5A). Within sleep, there was no difference in the percent of time spent in any state between groups (Figure 5B) and there was no difference in the number of transitions from either NREM sleep or REM sleep to waking (Figure 5C). That is, there was no increase in the number of arousals with LC stimulation. Finally, there was no rebound in sleep or change in percent spent in any sleep state on day 3 when no LC stimulation occurred.

However, LC sleep stimulation did cause decreases in CA1 spectral band power at several frequencies during specific sleep stages (Figures 5D and 5E). No change was seen in any band power during waking, although that is to be expected, as LC stimulation was turned off once signs of waking were observed. There was no LC-stimulation-associated change in higher frequency bands, such as slow gamma (30–50 Hz) or fast gamma (61–100 Hz) during any sleep state. However, both NREM slow wave sleep and NREM intermediate sleep showed a selective decrease in delta (1–4 Hz) band power during LC stimulation periods. The decrease in NREM-slow-wave sleep (SWS) delta power correlated with day 5 procedural errors on both the familiar and altered tasks (Table S1). Intermediate sleep also decreased band power in the frequency range associated with sleep spindles: sigma (10–15 Hz). During REM sleep, LC stimulation selectively decreased theta power (5–9 Hz; Figure 6A) and the percent drop in theta power correlated with overall day 5 performance. Theta power suppression accompanied day 5 procedural errors (i.e., errors at boxes that did not change between mazes) on both familiar and altered maze tasks but did not correlate with map errors (Table S1). Thus, NREM delta and REM sleep theta impairments corresponded with performance errors specifically in those areas of the maze that never changed their reward contingency. These types of errors can be associated with a general search pattern rather than reliance on a trusted map.

LC Stimulation Decreased Sleep Spindle Occurrence

In addition to frequency changes, we tested whether LC stimulation altered the rate of spindle occurrence during sleep following learning. Although there was no difference in baseline spindle occurrence between groups (ChR2− 0.045 ± 0.002 spindles/s; ChR2+ 0.055 ± 0.004 spindles/s), the percent change from baseline to day 1 sleep was significant between groups: ChR2+ rats experienced a decrease in spindle occurrence and ChR2− animals saw an increase (Figure 6B). LC stimulation reduced spindle occurrence in rats performing our learning task as well as in rats without a learning task (Figure 1D). The absence of a learning task significantly increased this reduction in spindle occurrence caused by LC stimulation (Figure S4). However, in both cohorts, when LC optogenetic stimulation occurred within a spindle, we found that spindle power decreased ~90 ms following light onset (Figure 6C). This 90-ms time frame is consistent with the conduction of LC action potentials through unmyelinated axons to their terminals [32, 33]. We found that the occurrence of spindles whose length exceeded our inter-stimulus interval, i.e., spindles ≥0.6 s in length, were disproportionately reduced, whereas shorter spindles were unaffected (Figure 6D). This change in spindle occurrence from baseline to day 1 correlated with overall day 5 performance on the altered and familiar tasks. The change in spindle occurrence specifically correlated with day 5 map errors on the familiar task (i.e., box positions that changed between mazes), but not with procedural errors (Table S1). That is, the rate of spindle occurrence was associated with disambiguating reward locations between the two tasks. As only long spindles were reduced, their reduction likely contributed to the confusion between familiar and altered locations.

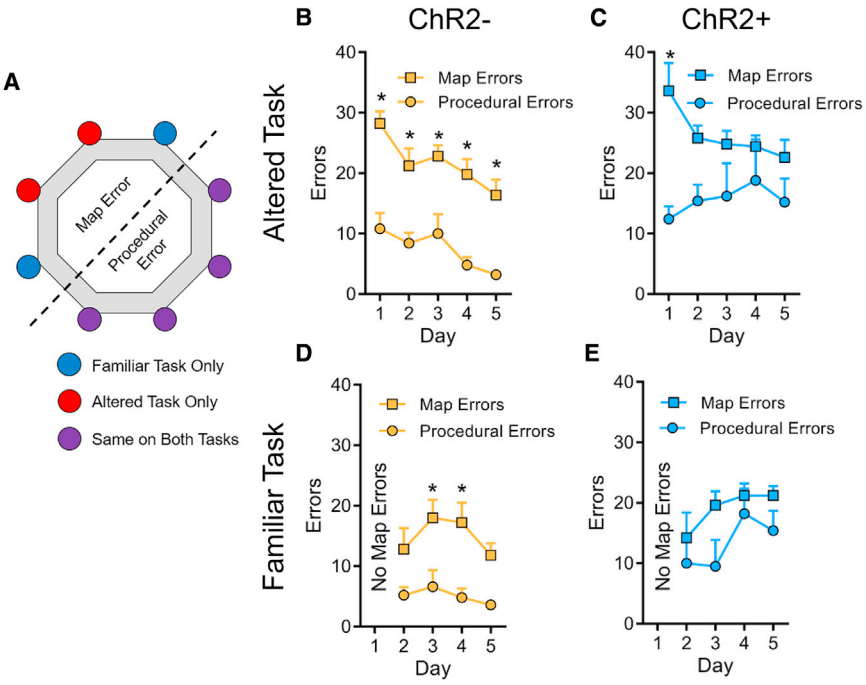

Figure 4. LC Stimulation during Sleep Alters Maze-Solving Strategies

(A) Schematic showing difference between procedural errors and map errors. Red dots would be map errors on the familiar task, as they are only baited during the altered task, and blue dots represent map errors on the altered task, as those boxes are only baited on the familiar task. Purple dots are boxes that are consistent, whether baited or non-baited, between the familiar and the altered task.

(B) ChR2− group performance on the altered task broken down by error type. Two-way ANOVA; Sidak post hoc: map versus procedural errors day 1 $p < 0.0001$; day 2 $p = 0.0012$; day 3 $p = 0.0012$; day 4 $p = 0.0001$; day 5 $p = 0.0009$. *$p < 0.005$.

(C) ChR2+ group performance on the altered task broken down by error type. Two-way ANOVA; Sidak post hoc: map versus procedural errors: day 1 $p = 0.0016$. *$p < 0.005$.

(D) ChR2− group performance on the familiar task broken down by error type. Two-way ANOVA; Sidak post hoc: map versus procedural errors day 3 $p = 0.01$; day 4 $p = 0.0047$. *$p < 0.05$.

(E) ChR2+ performance on the familiar task broken down by error type. Five rats in each group for (B)–(E) are shown. Symbols and error bars represent day mean ± SEM.

Aberrant LC Activity during Sleep Interfered with Ripple-Spindle Coupling

Previous work has posited that the coupling of ripples to spindles is important for learning and memory consolidation [1, 2]. Therefore, we examined whether LC stimulation had any effect on ripple-spindle coupling. During baseline sleep, there was no difference between groups in ripple-spindle coupling, and coupling was significantly non-random in both groups when tested against shuffled data (Figure 7A). However, during day 1 sleep with LC stimulation, ChR2+ rats had significantly decreased ripple-spindle coupling compared to ChR2- rats, although coupling was still non-random for both groups (Figure 7B). To ensure that this difference in coupling was not due to changes in CA1 ripple occurrence rate, we analyzed ripples and found that there was no change in ripple occurrence or the average length of ripples between groups or across days (Figures S5B–S5E), nor did ripples correlate with behavioral performance (Table S1). Moreover, ripple probability in relation to spindle onset was not different between groups on either day (Figure S5F). Therefore, this change in ripple-spindle coupling was likely due to the changes seen in spindles rather than ripples. Finally, the changes in coupling correlated with overall day 5 performance on both the altered and familiar tasks, and were associated with both map errors and procedural errors on the familiar task and with procedural errors on the altered task (Table S1).

DISCUSSION

Our present findings demonstrate that LC activity normally decreases to near-zero firing rate during spindle-rich NREM-intermediate sleep as well as REM sleep. We found that endogenous LC activity during a sleep spindle leads to spindle termination, and optogenetically enhanced LC activity during sleep reduces the rate of spindle occurrence, particularly in longer spindles, as well as power in the theta band during REM sleep and in the delta band during NREM sleep, while leaving sleep as a behavioral state intact. Further, LC stimulation during sleep following learning decreases the fidelity of hippocampal place encoding, while leaving hippocampal ripples and pyramidal cell activity rates unchanged. As a result, consolidation of spatial memory was also hampered, which led to rats utilizing non-hippocampal procedural strategies to solve the task. These alterations in learning strategies directly correlated with drops in sleep spindle occurrence and in REM sleep theta and NREM delta power, which were the result of LC stimulation during sleep. We believe the normal drop in LC activity prior to each sleep spindle and during REM sleep—although not required to maintain somnolence—is important for normal NREM sleep spindle generation, NREM delta and REM sleep theta power, and, by extension, hippocampal memory consolidation [11, 13].

Previous work has shown that the pressure for sleep spindles increases after learning and their increased occurrence correlates with memory consolidation [12, 22, 34]. Upregulation of sleep spindles improves memory [13, 35]. We found that LC stimulation without learning reduced the occurrence of sleep spindles more than 60%, and under the pressure of learning, LC stimulation significantly reduced spindles but to a lesser magnitude, possibly due to a training-induced spindle drive. Long spindles (>0.5 s) increased by almost 50% under learning conditions, but LC stimulation during sleep prevented such increase, instead reducing long spindles by ~20%, making the effective long spindle reduction roughly 70% under learning conditions. We provide here the first evidence that preventing an increase in sleep spindles following learning prevents consolidation of a new memory and reconsolidation of a familiar memory, with error types revealing deficits in the disambiguation of

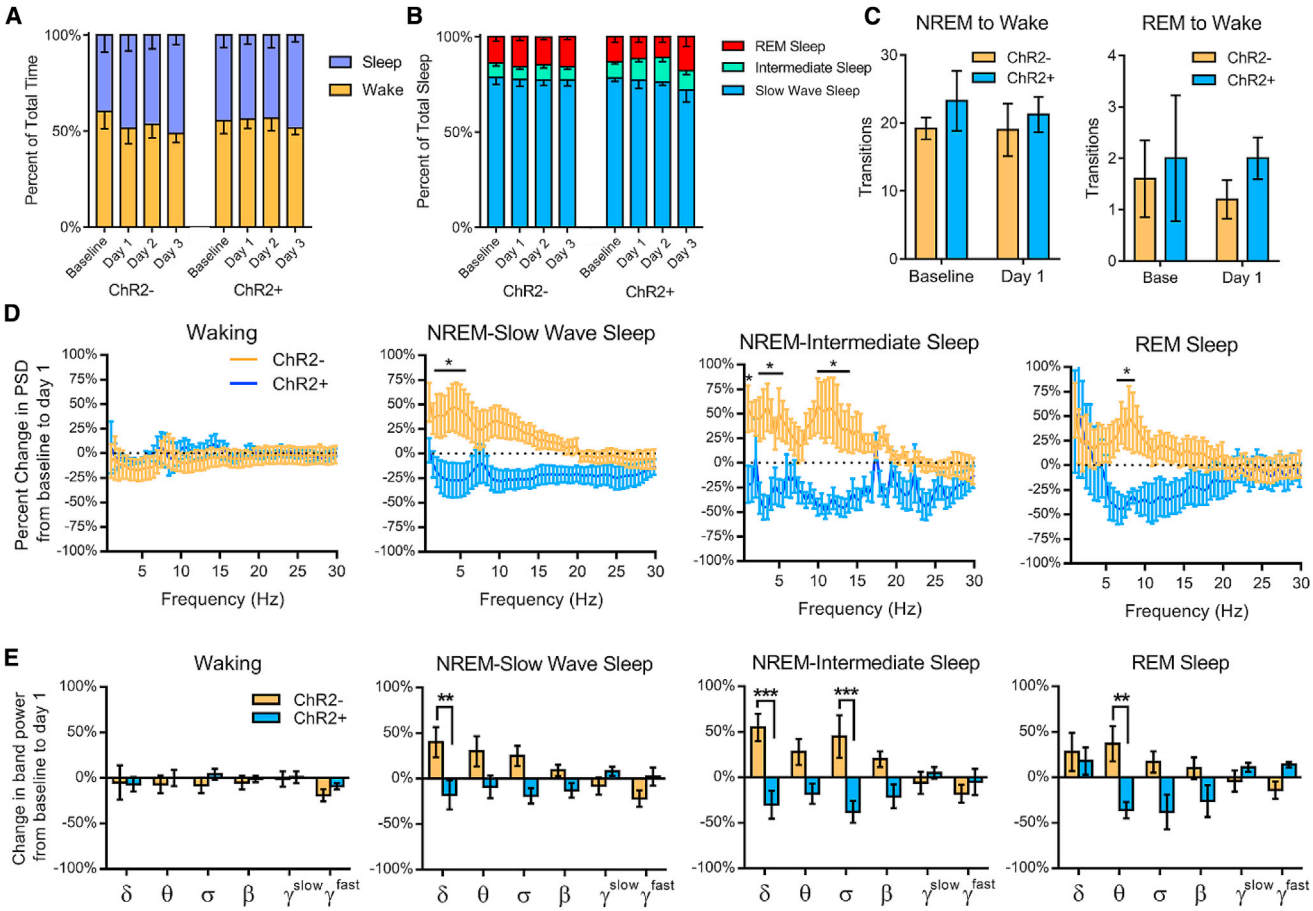

Figure 5. LC Stimulation Does Not Produce Changes in Sleep Architecture but Does Alter Spectral Power

(A) Mean (± SEM) percent time spent awake and sleeping compared to total time.

(B) Mean (± SEM) percent of total sleep spent in slow-wave sleep, intermediate sleep, and REM sleep.

(C) The mean (± SEM) number of transitions from non-REM (NREM) sleep to wake and from REM sleep to wake within the first hour of sleep.

(D) Percent change from baseline to day 1 in CA1 LFP spectral power during waking, slow-wave sleep, intermediate sleep, and REM sleep. Five ChR2- rats and four ChR2+ rats for (A)–(D) are shown. Two-way ANOVA; Sidak post hoc. Bars represent mean ± SEM.

(E) Percent change in band power from baseline to day 1 sleep. δ 1–4 Hz, θ 5–9 Hz, σ 10–15 Hz, β 16–20 Hz, γ^{slow} 30–50 Hz, γ^{fast} 61–100 Hz for all states. Two-way ANOVA; Sidak post hoc: slow wave sleep delta p = 0.0067; intermediate sleep delta p = 0.0007 sigma p = 0.0009; REM sleep theta p = 0.005.

*p < 0.05; **p < 0.01; ***p < 0.005.

information that distinguishes the two experiences. Further studies will be necessary to investigate the contribution of long spindles to the integration of new information into preexisting memory circuits.

Persistent LC activity reduced REM sleep theta power, which could have REM-sleep-dependent memory consolidation implications [25, 36]. REM sleep is a time of synaptic downscaling [37]. Norepinephrine blocks depotentiation [6, 38] and sleep-dependent synaptic downscaling [39]. Normally, place fields maintain stable place coding over weeks [30], despite backward expansion occurring during task performance [28], necessitating synaptic downscaling between sessions. We show that, when we sustain LC activity across sleep, place fields grow abnormally large across days, providing indirect evidence of unchecked LTP and a failure to depotentiate during REM sleep. These REM sleep disruption results support Boyce et al. [11], showing the importance of REM sleep theta for memory consolidation. We further provide indirect evidence of a possible depotentiation deficit underlying these consolidation errors.

In addition to decreasing sleep spindle occurrence and power and REM sleep theta power, 2-Hz LC stimulation also led to a significant decrease in slow-wave-delta power, which also correlated with the number of procedural errors on both tasks. Previous work in humans has highlighted the function of NREM slow waves in the consolidation of visual perceptual and implicit paired-associate learning [40, 41]. Artificial enhancement or disruption of slow waves has been shown to enhance paired-associate or impair motor skill memory consolidation, respectively [42, 43]. In rodents, LC neuron activity is shown to synchronize to the rising phase of slow waves [9]. It is possible that our manipulation of LC activity during sleep interferes with the timing of LC activity in relation to slow waves, which may result in decreased delta power or disrupt the effect of memory processing thought to occur during sharp-wave ripples at slow wave

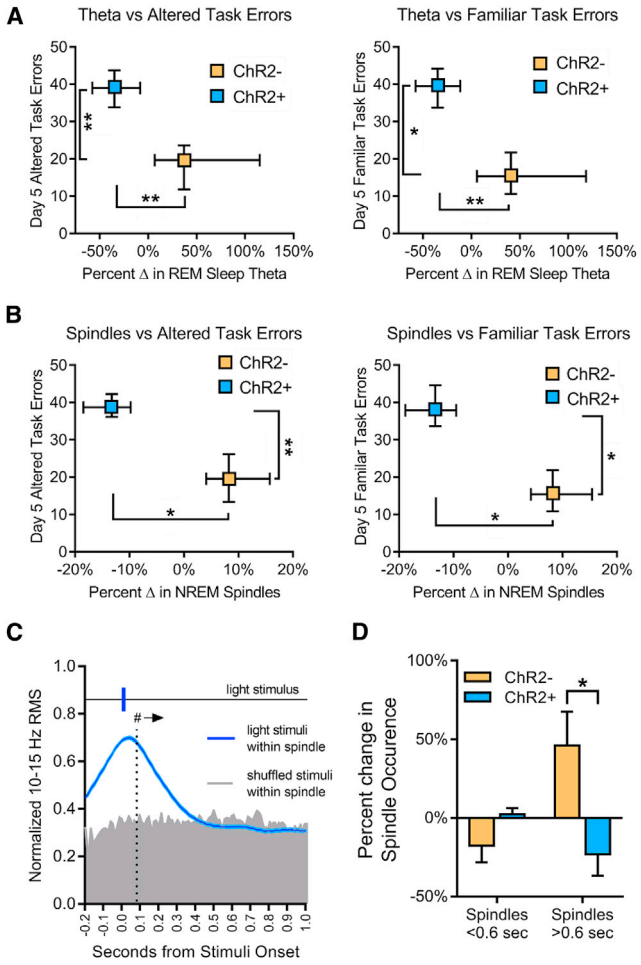

Figure 6. Changes in REM Sleep Theta Power and NREM Spindle Occurrence from Baseline Sleep to Day 1 Sleep with LC Stimulation

(A) The percent change from baseline to day 1 in REM sleep theta power versus day 5 altered task total errors (left) and day 5 familiar task total errors. ChR2+ versus ChR2− change in REM theta (x axis comparison) Mann-Whitney p = 0.0079. ChR2+ versus ChR2− altered task errors (y axis comparison) Mann-Whitney p = 0.008. ChR2+ versus ChR2− familiar task errors (y axis comparison) Mann-Whitney p = 0.016.

(B) The percent change from baseline to day 1 in CA1 spindle occurrence during NREM sleep versus day 5 altered task total errors (left) and day 5 familiar task total errors. ChR2+ versus ChR2− change in spindle rate (x axis comparison) Mann-Whitney p = 0.016. ChR2+ versus ChR2− altered task errors (y axis comparison) Mann-Whitney p = 0.008. ChR2+ versus ChR2− familiar task errors (y axis comparison) Mann-Whitney p = 0.016. Error bars represent the minimum and maximum within a dataset; vertical and horizontal lines cross at the mean from each group, marked with symbols for both (A) and (B).

(C) The effect of LC stimulation on mean (± SEM) CA1 sigma power within spindles. Normalized CA1 sigma power is shown in relation to light stimulation events within spindles (n = 700). Events were then shuffled within spindles to preserve spindle specificity for ten shuffled datasets of 700 shuffled events each. A two-way ANOVA, Sidak post hoc was calculated for the real data (n = 700 events) versus each shuffled set individually (n = 700 per set) and then against the average of all ten shuffles. The effect of light stimuli was non-random ($p < 0.05$ from shuffled) for t = −0.04–0.18 for all individual ANOVAs and the combined two-way ANOVAs. Light stimulation significantly reduced sigma RMS; two-way ANOVA; Dunnett post hoc light onset t = 0 versus t > 0. #$p < 0.05$ at t = 0.088 s (dashed line) and onward.

(D) The percent change in occurrence of spindles greater or less than 0.6 s in length. Two-way ANOVA; Sidak post hoc ChR2− versus ChR2+ p = 0.013. Data are displayed as mean ± SEM.

*$p < 0.05$; **$p < 0.01$. See also Figure S4 and Table S1.

peaks. More work is necessary to understand the relationship between NREM slow waves and LC activity in relation to memory consolidation.

Although previous work has highlighted the importance of noradrenergic activity in memory formation during waking [44–47], little has been done to examine what function the presence or, especially, the absence of norepinephrine during sleep may have on learning and memory. Further work is needed to understand whether the effects of aberrant LC activity during sleep on hippocampal spatial encoding and memory are due to noradrenergic receptor activation or to dopamine, which is released from the same terminals when norepinephrine is depleted [48, 49]. The low stimulation rate used in our study makes dopaminergic mechanisms less likely.

An interesting facet of our results is the persistence of rodent behavioral performance deficits despite cessation of LC optogenetic stimulation. Although stimulation ceases after day 2, the ChR2+ rats' performance continues to decline. The initial decrease in performance up to day 3 in both ChR2− and ChR2+ rats on the familiar task may be due to the interference of information from the altered task on familiar task performance. Then, ChR2− rats' performance improves due to the use of efficient spatial strategies from healthy hippocampal function. However, the adaptation of ChR2+ rats to disrupted hippocampal place cell encoding is to adopt a performance strategy that does not require hippocampal spatial mapping. After day 3, this inefficient procedural strategy produces a behavioral deficit relative to the improving ChR2− controls. We postulate that ChR2+ rats do not return to a hippocampal strategy, as there is little motivation to attempt a strategy shift; i.e., despite frequent errors, they consume the same number of rewards. Long-term hippocampal impairment is not a factor; once the formerly LC stimulated ChR2+ rats were introduced to another hippocampus-dependent task in a different context (the novel task), they were able to learn the task at similar rates to ChR2− rats. Future work is needed to understand why only 2 days of post-learning abnormal LC activity during sleep caused lasting but context-specific hippocampal deficits.

We propose that LC silences permit sleep spindle generation by preventing noradrenergic depolarization of thalamocortical circuits as depolarization prevents the calcium spikes necessary for spindle generation [20]. Persistent LC activity, as in our study, would decrease spindle occurrence, thereby reducing spindle-ripple-related neural activity. Higher frequencies of LC stimulation during sleep used in another study also suppressed ripple-spindle events [50]. LC silences prior to spindles could be key to ripple-spindle coupling and inter-regional communication during memory consolidation [1, 2].

We have shown profound learning and memory reconsolidation behavioral deficits with a mild physiological increase in LC cell activity during the sleep consolidation period. We also show subsequent neural coding instability. Together, these results likely explain the animals' inability to use a neural code to

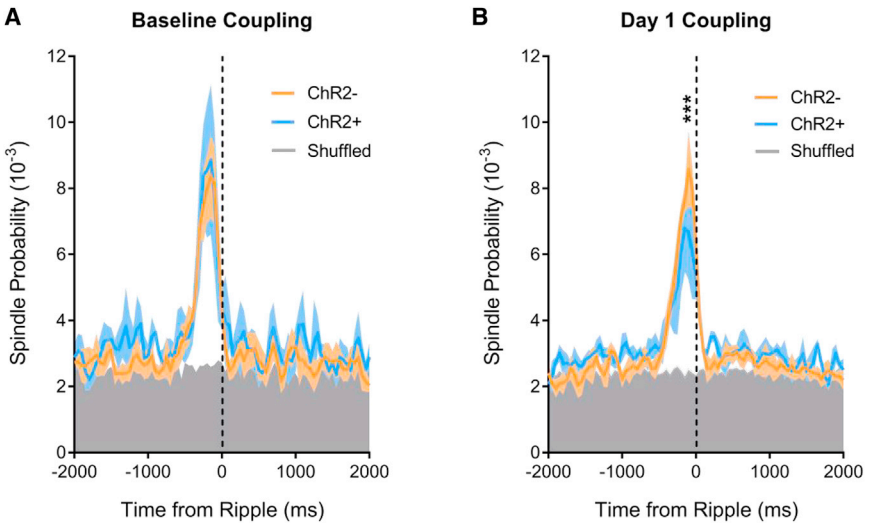

Figure 7. LC Stimulation during Sleep Interferes with Ripple-Spindle Coupling

(A) Spindle onset mean (± SEM) probability displayed with respect to ripple onset at t = 0 during baseline sleep (no LC stimulation in either group). Ripple onset timestamps were shuffled within NREM sleep periods with no repeating timestamps within trials and were shuffled for a total of 15 trials to ensure coupling was non-random. Two-way ANOVA; Sidak post hoc; ChR2+ versus ChR2+ shuffled $p < 0.0001$; ChR2− versus ChR2− shuffled $p < 0.0001$. There was no difference between the shuffled values for ChR2+ and ChR2− groups ($p = 0.997$); therefore, only ChR2+ shuffled values (in gray region) are displayed for visual purposes. Any value within the gray region represents random probability for both ChR2+ and ChR2−.

(B) Spindle onset probability displayed with respect to ripple onset at t = 0 during day 1 sleep with 2-Hz LC stimulation. Two-way ANOVA; Sidak post hoc; ChR2+ versus ChR2+ shuffled $p < 0.0001$; ChR2− versus ChR2− shuffled $p < 0.0001$. ChR2− versus ChR2+ significant difference from t = −50 to −250 ms $p < 0.0001$. ChR2− n = 4; ChR2+ n = 5; ***$p < 0.0001$. As there was no difference between either group's shuffled data in (B) as well ($p = 0.958$), within (B) the gray region represents both ChR2+ and ChR2− shuffled data. Data are displayed as mean (colored line) ± SEM (same-colored shaded region).
See also Figure S5.

solve the spatial memory task. More work is required to study the replay patterns and plasticity effects of inappropriate LC activity during sleep consolidation.

In light of our current data, we conclude that LC silences play an important role in spindle generation and ripple-spindle coupling, as well as in normal NREM delta and REM sleep theta rhythm power—oscillations essential to normal offline processing of memory [11, 51, 52]. Our research suggests that LC activity, or lack thereof, during sleep may play a role in memory expression and be related to memory issues in conditions of abnormal LC activity during sleep, such as post-traumatic stress disorder and Alzheimer's disease [53, 54].

STAR★METHODS

Detailed methods are provided in the online version of this paper and include the following:

- KEY RESOURCES TABLE
- CONTACT FOR REAGENT AND RESOURCE SHARING
- EXPERIMENTAL MODELS AND SUBJECT DETAILS
- METHOD DETAILS
  - Viral Injection
  - Electrode Implantation
  - Behavioral Training and Motivation
  - Behavioral Protocol and Rectangular Maze
  - Electrophysiological Recording
  - LC Optical Stimulation
  - LC Stimulation and Arousal Experiments
  - Histology
- QUANTIFICATION AND STATISTICAL ANALYSIS
  - Behavioral Task Performance
  - Sleep State Analysis
  - Power Spectral Band Analysis
  - Sleep Spindle and Ripple Identification
  - Ripple-Spindle Coupling
  - Single Unit Isolation
  - Place Cell Identification and Analysis

SUPPLEMENTAL INFORMATION

Supplemental Information includes five figures and one table and can be found with this article online at https://doi.org/10.1016/j.cub.2018.09.054.

ACKNOWLEDGMENTS

We thank Jill Priestley for conducting initial pilot studies, Emily Pickup for animal assistance, and Karl Deisseroth for experimental advice. Funding for this research was provided by NIMH R01 60670 (G.R.P.), br088373 Wellcome Senior Clinical fellowship (A.E.P.), and K.M.S. was supported by the University of Michigan Systems and Integrative Biology T32.

AUTHOR CONTRIBUTIONS

K.M.S. and G.R.P. designed experiments; E.M.V., G.A.-J., Y.L., and A.E.P. constructed and provided vectors; K.M.S., D.S.B., and K.J.D.C. performed experiments; S.J.S. contributed experimental and data analysis expertise; K.M.S., B.A.G., and M.A.F. analyzed data; and K.M.S. and G.R.P. wrote the manuscript.

DECLARATION OF INTERESTS

The authors declare no competing interests.

Received: April 29, 2018
Revised: July 10, 2018
Accepted: September 25, 2018
Published: November 1, 2018

REFERENCES

1. Wierzynski, C.M., Lubenov, E.V., Gu, M., and Siapas, A.G. (2009). State-dependent spike-timing relationships between hippocampal and prefrontal circuits during sleep. Neuron *61*, 587–596.

2. Siapas, A.G., and Wilson, M.A. (1998). Coordinated interactions between hippocampal ripples and cortical spindles during slow-wave sleep. Neuron *21*, 1123–1128.
3. Sirota, A., Csicsvari, J., Buhl, D., and Buzsáki, G. (2003). Communication between neocortex and hippocampus during sleep in rodents. Proc. Natl. Acad. Sci. USA *100*, 2065–2069.
4. Ji, D., and Wilson, M.A. (2007). Coordinated memory replay in the visual cortex and hippocampus during sleep. Nat. Neurosci. *10*, 100–107.
5. Sara, S.J. (2009). The locus coeruleus and noradrenergic modulation of cognition. Nat. Rev. Neurosci. *10*, 211–223.
6. O'Dell, T.J., Connor, S.A., Guglietta, R., and Nguyen, P.V. (2015). β-adrenergic receptor signaling and modulation of long-term potentiation in the mammalian hippocampus. Learn. Mem. *22*, 461–471.
7. Carter, M.E., Yizhar, O., Chikahisa, S., Nguyen, H., Adamantidis, A., Nishino, S., Deisseroth, K., and de Lecea, L. (2010). Tuning arousal with optogenetic modulation of locus coeruleus neurons. Nat. Neurosci. *13*, 1526–1533.
8. Eschenko, O., and Sara, S.J. (2008). Learning-dependent, transient increase of activity in noradrenergic neurons of locus coeruleus during slow wave sleep in the rat: brain stem-cortex interplay for memory consolidation? Cereb. Cortex *18*, 2596–2603.
9. Eschenko, O., Magri, C., Panzeri, S., and Sara, S.J. (2012). Noradrenergic neurons of the locus coeruleus are phase locked to cortical up-down states during sleep. Cereb. Cortex *22*, 426–435.
10. Aston-Jones, G., and Bloom, F.E. (1981). Activity of norepinephrine-containing locus coeruleus neurons in behaving rats anticipates fluctuations in the sleep-waking cycle. J. Neurosci. *1*, 876–886.
11. Boyce, R., Glasgow, S.D., Williams, S., and Adamantidis, A. (2016). Causal evidence for the role of REM sleep theta rhythm in contextual memory consolidation. Science *352*, 812–816.
12. Nishida, M., and Walker, M.P. (2007). Daytime naps, motor memory consolidation and regionally specific sleep spindles. PLoS ONE *2*, e341.
13. Mednick, S.C., McDevitt, E.A., Walsh, J.K., Wamsley, E., Paulus, M., Kanady, J.C., and Drummond, S.P.A. (2013). The critical role of sleep spindles in hippocampal-dependent memory: a pharmacology study. J. Neurosci. *33*, 4494–4504.
14. Sara, S.J. (2017). Sleep to remember. J. Neurosci. *37*, 457–463.
15. Braunewell, K.H., and Manahan-Vaughan, D. (2001). Long-term depression: a cellular basis for learning? Rev. Neurosci. *12*, 121–140.
16. Manahan-Vaughan, D., and Braunewell, K.-H. (1999). Novelty acquisition is associated with induction of hippocampal long-term depression. Proc. Natl. Acad. Sci. USA *96*, 8739–8744.
17. Watts, A., Gritton, H.J., Sweigart, J., and Poe, G.R. (2012). Antidepressant suppression of non-REM sleep spindles and REM sleep impairs hippocampus-dependent learning while augmenting striatum-dependent learning. J. Neurosci. *32*, 13411–13420.
18. Gottesmann, C. (1992). Detection of seven sleep-waking stages in the rat. Neurosci. Biobehav. Rev. *16*, 31–38.
19. Steriade, M., McCormick, D.A., and Sejnowski, T.J. (1993). Thalamocortical oscillations in the sleeping and aroused brain. Science *262*, 679–685.
20. Lee, K.H., and McCormick, D.A. (1996). Abolition of spindle oscillations by serotonin and norepinephrine in the ferret lateral geniculate and perigeniculate nuclei in vitro. Neuron *17*, 309–321.
21. Li, Y., Hickey, L., Perrins, R., Werlen, E., Patel, A.A., Hirschberg, S., Jones, M.W., Salinas, S., Kremer, E.J., and Pickering, A.E. (2016). Retrograde optogenetic characterization of the pontospinal module of the locus coeruleus with a canine adenoviral vector. Brain Res. *1641* (Pt B), 274–290.
22. Tamminen, J., Payne, J.D., Stickgold, R., Wamsley, E.J., and Gaskell, M.G. (2010). Sleep spindle activity is associated with the integration of new memories and existing knowledge. J. Neurosci. *30*, 14356–14360.
23. Poe, G.R., Thompson, C.M., Riley, B.T., Tysor, M.K., Bjorness, T.E., Steinhoff, B.P., and Ferluga, E.D. (2002). A spatial memory task appropriate for electrophysiological recordings. J. Neurosci. Methods *121*, 65–74.
24. Abel, T., Havekes, R., Saletin, J.M., and Walker, M.P. (2013). Sleep, plasticity and memory from molecules to whole-brain networks. Curr. Biol. *23*, R774–R788.
25. Poe, G.R., Nitz, D.A., McNaughton, B.L., and Barnes, C.A. (2000). Experience-dependent phase-reversal of hippocampal neuron firing during REM sleep. Brain Res. *855*, 176–180.
26. Booth, V., and Poe, G.R. (2006). Input source and strength influences overall firing phase of model hippocampal CA1 pyramidal cells during theta: relevance to REM sleep reactivation and memory consolidation. Hippocampus *16*, 161–173.
27. Mehta, M.R., Barnes, C.A., and McNaughton, B.L. (1997). Experience-dependent, asymmetric expansion of hippocampal place fields. Proc. Natl. Acad. Sci. USA *94*, 8918–8921.
28. Mehta, M.R., Quirk, M.C., and Wilson, M.A. (2000). Experience-dependent asymmetric shape of hippocampal receptive fields. Neuron *25*, 707–715.
29. Ekstrom, A.D., Meltzer, J., McNaughton, B.L., and Barnes, C.A. (2001). NMDA receptor antagonism blocks experience-dependent expansion of hippocampal "place fields". Neuron *31*, 631–638.
30. Thompson, L.T., and Best, P.J. (1990). Long-term stability of the place-field activity of single units recorded from the dorsal hippocampus of freely behaving rats. Brain Res. *509*, 299–308.
31. Bjorness, T.E., Riley, B.T., Tysor, M.K., and Poe, G.R. (2005). REM restriction persistently alters strategy used to solve a spatial task. Learn. Mem. *12*, 352–359.
32. Aston-Jones, G., Segal, M., and Bloom, F.E. (1980). Brain aminergic axons exhibit marked variability in conduction velocity. Brain Res. *195*, 215–222.
33. Aston-Jones, G., Foote, S.L., and Segal, M. (1985). Impulse conduction properties of noradrenergic locus coeruleus axons projecting to monkey cerebrocortex. Neuroscience *15*, 765–777.
34. Eschenko, O., Mölle, M., Born, J., and Sara, S.J. (2006). Elevated sleep spindle density after learning or after retrieval in rats. J. Neurosci. *26*, 12914–12920.
35. Kaestner, E.J., Wixted, J.T., and Mednick, S.C. (2013). Pharmacologically increasing sleep spindles enhances recognition for negative and high-arousal memories. J. Cogn. Neurosci. *25*, 1597–1610.
36. Poe, G.R. (2017). Sleep is for forgetting. J. Neurosci. *37*, 464–473.
37. Li, W., Ma, L., Yang, G., and Gan, W.B. (2017). REM sleep selectively prunes and maintains new synapses in development and learning. Nat. Neurosci. *20*, 427–437.
38. Katsuki, H., Izumi, Y., and Zorumski, C.F. (1997). Noradrenergic regulation of synaptic plasticity in the hippocampal CA1 region. J. Neurophysiol. *77*, 3013–3020.
39. Diering, G.H., Nirujogi, R.S., Roth, R.H., Worley, P.F., Pandey, A., and Huganir, R.L. (2017). Homer1a drives homeostatic scaling-down of excitatory synapses during sleep. Science *355*, 511–515.
40. Stickgold, R., Whidbee, D., Schirmer, B., Patel, V., and Hobson, J.A. (2000). Visual discrimination task improvement: a multi-step process occurring during sleep. J. Cogn. Neurosci. *12*, 246–254.
41. Mölle, M., Marshall, L., Gais, S., and Born, J. (2004). Learning increases human electroencephalographic coherence during subsequent slow sleep oscillations. Proc. Natl. Acad. Sci. USA *101*, 13963–13968.
42. Marshall, L., Helgadóttir, H., Mölle, M., and Born, J. (2006). Boosting slow oscillations during sleep potentiates memory. Nature *444*, 610–613.
43. Fattinger, S., de Beukelaar, T.T., Ruddy, K.L., Volk, C., Heyse, N.C., Herbst, J.A., Hahnloser, R.H.R., Wenderoth, N., and Huber, R. (2017). Deep sleep maintains learning efficiency of the human brain. Nat. Commun. *8*, 15405.
44. Cahill, L., Prins, B., Weber, M., and McGaugh, J.L. (1994). Beta-adrenergic activation and memory for emotional events. Nature *371*, 702–704.
45. Gazarini, L., Stern, C.A.J., Carobrez, A.P., and Bertoglio, L.J. (2013). Enhanced noradrenergic activity potentiates fear memory consolidation

and reconsolidation by differentially recruiting α1- and β-adrenergic receptors. Learn. Mem. *20*, 210–219.

46. Roozendaal, B., Nguyen, B.T., Power, A.E., and McGaugh, J.L. (1999). Basolateral amygdala noradrenergic influence enables enhancement of memory consolidation induced by hippocampal glucocorticoid receptor activation. Proc. Natl. Acad. Sci. USA *96*, 11642–11647.
47. Przybyslawski, J., Roullet, P., and Sara, S.J. (1999). Attenuation of emotional and nonemotional memories after their reactivation: role of beta adrenergic receptors. J. Neurosci. *19*, 6623–6628.
48. Kempadoo, K.A., Mosharov, E.V., Choi, S.J., Sulzer, D., and Kandel, E.R. (2016). Dopamine release from the locus coeruleus to the dorsal hippocampus promotes spatial learning and memory. Proc. Natl. Acad. Sci. USA *113*, 14835–14840.
49. Wagatsuma, A., Okuyama, T., Sun, C., Smith, L.M., Abe, K., and Tonegawa, S. (2018). Locus coeruleus input to hippocampal CA3 drives single-trial learning of a novel context. Proc. Natl. Acad. Sci. USA *115*, E310–E316.
50. Novitskaya, Y., Sara, S.J., Logothetis, N.K., and Eschenko, O. (2016). Ripple-triggered stimulation of the locus coeruleus during post-learning sleep disrupts ripple/spindle coupling and impairs memory consolidation. Learn. Mem. *23*, 238–248.
51. Maingret, N., Girardeau, G., Todorova, R., Goutierre, M., and Zugaro, M. (2016). Hippocampo-cortical coupling mediates memory consolidation during sleep. Nat. Neurosci. *19*, 959–964.
52. Walker, M.P. (2009). The role of slow wave sleep in memory processing. J. Clin. Sleep Med. *5* (2, Suppl), S20–S26.
53. Berridge, C.W., and Waterhouse, B.D. (2003). The locus coeruleus-noradrenergic system: modulation of behavioral state and state-dependent cognitive processes. Brain Res. Brain Res. Rev. *42*, 33–84.
54. Mellman, T.A., Kumar, A., Kulick-Bell, R., Kumar, M., and Nolan, B. (1995). Nocturnal/daytime urine noradrenergic measures and sleep in combat-related PTSD. Biol. Psychiatry *38*, 174–179.
55. Sara, S., and Segal, M. (1991). Plasticity of sensory responses of locus coeruleus neurons in the behaving rat: implications for cognition. Prog. Brain Res. *88*, 571–585.
56. Ghasemi, A., and Zahediasl, S. (2012). Normality tests for statistical analysis: a guide for non-statisticians. Int. J. Endocrinol. Metab. *10*, 486–489.
57. Emrick, J.J., Gross, B.A., Riley, B.T., and Poe, G.R. (2016). Different simultaneous sleep states in the hippocampus and neocortex. Sleep *39*, 2201–2209.
58. Gross, B.A., Walsh, C.M., Turakhia, A.A., Booth, V., Mashour, G., and Poe, G.R. (2009). Open-source logic-based automated sleep scoring software using electrophysiological recordings in rats. J. Neurosci. Methods *184*, 10–18.
59. Girardeau, G., Benchenane, K., Wiener, S.I., Buzsáki, G., and Zugaro, M.B. (2009). Selective suppression of hippocampal ripples impairs spatial memory. Nat. Neurosci. *12*, 1222–1223.
60. Skaggs, W.E., McNaughton, B.L., Gothard, K.M., and Markus, E.J. (1993). An Information-Theoretic Approach to Deciphering the Hippocampal Code. Proceedings of Advances in Neural Information Processing Systems 5 (Morgan Kaufmann), pp. 1030–1037.
61. Fuhs, M.C., Vanrhoads, S.R., Casale, A.E., McNaughton, B., and Touretzky, D.S. (2005). Influence of path integration versus environmental orientation on place cell remapping between visually identical environments. J. Neurophysiol. *94*, 2603–2616.
62. Roux, L., Hu, B., Eichler, R., Stark, E., and Buzsáki, G. (2017). Sharp wave ripples during learning stabilize the hippocampal spatial map. Nat. Neurosci. *20*, 845–853.

STAR★METHODS

KEY RESOURCES TABLE

REAGENT or RESOURCE	SOURCE	IDENTIFIER
Antibodies		
Mouse monoclonal anti-Tyrosine Hydroxylase	Immunostar	Cat#: 22941; RRID: AB_572268
Rabbit polyclonal anti-mCherry	Biovision	Cat#: 5993-100
Goat AlexaFluor488 anti-mouse	Fisher	RRID: AB_2633275
Goat AlexaFluor594 anti-rabbit	Fisher	RRID: AB_2534095
Bacterial and Virus Strains		
CAV2-PRSX8-ChR2-mCherry	Plateforme de Vecterologie de Montipellier, Institut de Genetique Moleculaire de Montpellier CNRS UMR 5535	N/A
Lenti-PRSX8-ChR2-mCherry	University of Pennsylvania Vector Core	N/A
Chemicals, Peptides, and Recombinant Proteins		
Isoflurane	Zoetis	N/A
10% Formalin	VWR	N/A
Prolong Gold Antifade Agent	Invitrogen/Fisher	Cat#: P36930; RRID: SCR_015961
Experimental Models: Organisms/Strains		
Long-Evans Male Rats	Charles-River	Strain Code:006
Software and Algorithms		
MATLAB v 2017a	Mathworks	RRID:SCR_001622
Offline Sorter 3D v 3.3.2	Plexon	RRID:SCR_000012
NeuroExplorer 5	Neuroexplorer	RRID:SCR_001818
Prism 7	Graphpad	RRID:SCR_002798
Other		
Stereotaxic Apparatus	World Precision Instruments	N/A
Tetrode Wire	Sandvik	Cat#: PX000029
Stainless steel EMG wire	Cooner Wire	Cat#: AS636
Ground Screws	Invivo1	Cat#: E363/20/SPC
Digital Lynx	Neuralynx	DigitalLynx 4SX Upgrade
Cryostat	Leica	CM 1950
Fluorescent Microscope/Camera	Olympus	BX-51

CONTACT FOR REAGENT AND RESOURCE SHARING

Further information and request for resources may be directed to the Lead Contact, Gina R. Poe (ginapoe@ucla.edu).

EXPERIMENTAL MODELS AND SUBJECT DETAILS

A total of twenty-six male Long-Evans rats (Charles River), age 4-5 months and weighing approximately 350-400 g were individually housed in cages (45.7 × 24.1 × 20.3 cm) with shaved cellulose bedding, climate controlled (23 ± 3°C and 40 ± 10% humidity) and with 12:12 hour light/dark cycle. Food and water were available *ad libitum* prior to food restriction during behavioral training. All animal procedures were carried out in accordance with the National Institutes of Health Guide for the Care and Use of Laboratory Animals and in accordance with the University of Michigan Committee on the Use and Care of Laboratory Animals.

METHOD DETAILS

Viral Injection

Animals were orally administered (20 mg/kg) ciprofloxacin and liquid acetaminophen (orally 30ml/150 mL water) 24 hours prior to surgery. Rats were anesthetized with isoflurane vapor (4% induction, 1%–2% maintenance) and placed in a stereotaxic frame. All

stereotaxic measurements were from bregma. A vector expressing a light sensitive channelrhodopsin-2 (ChR2) under the control of PRSx8 (synthetic dopamine beta hydroxylase promoter), lenti-PRSx8-ChR2-mCherry or CAV2-PRSx8-ChR2-mCherry [21], or a control vector, AAV-PRSx8-mCherry, was bilaterally injected (1.2 μl) into the locus coeruleus (AP −12.1 mm; ML ± 1.3mm; DV 6.1 mm at 20°) through 30-gauge injection cannula at a rate of 0.2 mL min^{-1} for 6 minutes. Post-injection, needles were left in tissue for 10 minutes prior to removal.

Electrode Implantation

LC and CA1 single cell recordings were collected with dual eight independently movable tetrodes (groups of four twisted microwires) microdrives. The anterior microdrive contained two bilateral cannula containing four tetrodes each targeting the hippocampus (from bregma: −4.0 mm AP; ± 2.5 mm ML; - 2.0–2.5 mm DV). The posterior microdrive contained two bilateral cannula containing four tetrodes each targeting the LC (from bregma: AP −12.1 mm; mediolateral ML ± 1.2mm; DV −6.1 mm at 20° to avoid the transverse sinus). A screw electrode (Plastics One) was implanted over the prefrontal cortex (from bregma: +2.0 mm AP; ± 2.0 mm ML) to be used as a ground. Two nuchal electromyographic (EMG) electrodes were implanted into the dorsal neck muscles. All implanted tetrodes were used to measure local field potential (LFP) and detect single unit activity. Anchor screws and dental cement were used to adhere implants to the skull.

Behavioral Training and Motivation

Rats were trained on an octagonal version of an eight-box spatial learning task originally developed in our lab [23]. Eight boxes were positioned with one at each corner of an elevated octagonal track. Each box consisted of a reward reservoir that is hidden behind a hinged door that must be opened to reach the food reward (Ensure® Abbott Labs, Columbus, OH). Each reservoir was fed by a plastic tube coupled to a syringe allowing the observer to fill reservoirs without interacting with the maze. Below each box, an inaccessible compartment was baited with Ensure so that all boxes smelled as though they contain a reward to prevent use of olfaction to locate the reward.

Rats were food restricted to > 85% of their free feeding weight and trained daily at ZT 0.5 (30 minutes into the light phase) in 30 minute sessions. Rats were trained to run clockwise on the track and locate the three of eight boxes that contained a food reward (0.5 mL Ensure) using static visual cues in the room. A training session consisted of three 5-lap trials (totaling 15 laps). Following a trial of five complete laps, the animal was removed from the maze and placed in a towel lined box for two minutes to encourage animals to use hippocampal-dependent learning and not working memory. During these two minutes, reservoirs were cleaned of food residue, and the maze was rotated (minimum 45 degrees, max 180 degrees). In all trials, reward boxes were located at the same allocentric locations with respect to visual cues of the room. At the beginning of each trial, rats were reintroduced to the maze at different locations to prevent learning reward location relative to initial placement on the maze.

Rats were trained on this familiar layout until they reached the defined performance threshold criterion of averaging less than one error per lap (16.1 ± 1.2 days). Errors consisted of skipping a reward box and checking a non-reward box. Animals were then implanted as described in *Electrode Implantation,* above. Following 10 days of surgical recovery in their home cages, animals were reintroduced to the maze with the familiar layout, now tethered for electrophysiological recording, and retrained until they met the performance criterion threshold again.

Behavioral Protocol and Rectangular Maze

The experimental protocol consisted of rats running 15 laps on the familiar layout, followed by a 20-minute break from the maze in a towel lined box. Light intensity in the room was kept low during running to minimize animal anxiety and optimize video tracking of the animal through headstage-mounted LEDs. Light was increased during the break between mazes as a cue for maze change. After the break, the lights were returned to low intensity and rats were run 15 laps in three trials on the altered maze where two of the three previous locations of the food were changed. In addition to counting total errors per lap, error type was also characterized. As two box positions changed between familiar and altered mazes, there are four potential errors that could be made at those four boxes and they were termed ''maze choice'' errors. Four potential ''procedural errors'' could be made at the four box positions that were never changed between mazes. Thus the probability of either error type being made at random on either the familiar or altered mazes is 0.5. Errors occurring at positions that remained static between mazes indicate an impaired hippocampal-dependent memory or perhaps abandonment of the hippocampal spatial strategy, whereas errors at baited positions that alternated between familiar and altered mazes indicate confusion between familiar and reversal maze maps. This 15-lap familiar, 20-minute break, 15-lap altered was run days 1-5.

Rats were given a break from running on days 6 and 7 and fed their normal restrictive diet. Day 8-10, animals were run on a rectangular maze with eight boxes [23], three of which contained food, similar to the days 1-5 exercise, only in a different room with different visual cues. Animals were run for three days to determine their ability to learn a new maze to the same criterion of less than one error per lap.

Electrophysiological Recording

Electrode data were recorded at a sampling rate of 32 kHz using Neuralynx Digital Lynx system (Neuralynx, Bozeman, MT). Hippocampal CA1 spikes were detected in real-time from 600 Hz to 6 kHz filtered continuously sampled tetrode data using amplitude threshold crossing. LC spikes were detected in the same manner, but with a 300 Hz to 6 kHz filter.

Tetrode placement in CA1 of the hippocampus was confirmed by moveable tetrode depth, as well as by waveform shape, frequency and audio-converted sound of pyramidal neural spikes. Tetrode placement in the LC was confirmed using calculated moveable tetrode depth, LC firing frequency i.e., relatively low firing during waking and silent during REM sleep quiescence [10], responsiveness to acoustic and/or tactile stimuli [55], and broad action potential waveform shape.

LC Optical Stimulation

All photostimulation experiments were conducted bilaterally. Two high powered blue LEDs (470 nm Luxeon) were coupled to optical fibers (200 mm core diameter, ThorLabs) using clear optical-grade epoxy (EPOTECH spectral transparency > 99% 380-980 nm) and implanted targeting the LC (same coordinates as tetrodes). Light pulses from LEDs were generated using a waveform generator (Agilent 3320A arbitrary waveform generator). Generated light pulses were 15 msec in duration and had a consistent 5-10 mW intensity at the fiber tip prior to implantation. *In vivo* confirmation of light evoked potentials from ChR2 expressing LC cells was confirmed with LC tetrode recordings (Figure S2B).

LC Stimulation and Arousal Experiments

Frequencies 4 Hz and above of LC optogenetic stimulation during NREM sleep decreased the animal's latency to arousal. SI Appendix Figure S2C shows example LFP spectral heatmaps and EMG traces in response to light stimulation during NREM sleep in ChR2- and a ChR2+ rats. Only ChR2+ rats awakened from NREM sleep, and the effect only occurred in response to light stimulation at 4 Hz frequencies or greater, which was confirmed by increased EMG activity and a power spectral density shift from slow wave delta power (0.4-4 Hz) to waking theta power (5-9 Hz) in the hippocampal CA1 LFP (Figure S2C middle). Light pulses at any frequency were insufficient to produced arousal in ChR2- rats. 1-3 Hz LC stimulation was incapable of awakening the ChR2+ rats from NREM sleep (Figure S2D). We therefore chose a 2 Hz LC stimulation frequency in order to maintain sleep continuity and avoid inducing arousals in ChR2+ rats, a sub-arousal threshold frequency that we used in all subsequent experiments. As spontaneous LC firing rates vary from 0-20 Hz, our evoked < 2 Hz activity rate was well within physiological parameters and similar to previous work [7].

Histology

Rats were anesthetized with 1.0 mL sodium pentobarbital (intraperitoneal injection), then transcardially perfused through the left ventricle with 150 mL phosphate buffered saline (1X PBS) followed by 150 mL 10% formalin. The brain was removed and placed in 10% formalin for 24 hours, and then in 1x PBS solution containing 30% sucrose for 48-72 hours. Brains were sectioned into 50 μm coronal sections on a cryostat and then washed for 10 min in 1x PBS three times. The sections were blocked for 30 min in a solution containing 0.5% Triton, followed by 30 min in 5% normal goat serum. Primary antibodies for tyrosine hydroxylase (TH), 1:500 mouse-anti-TH (Immunostar), and mCherry (1:500, rabbit anti-mCherry; Biovision) were applied for 24 hours at 4°C, followed by 1 hour at room temperature (~23°C). After three 10-min washes with 1X PBS, secondary antibodies (1:1000, Goat anti-Rabbit AlexaFluor-594 and 1:1000, Goat anti-Mouse AlexaFluor-488, Fisher) were applied for 24 hours at 4°C. After three 10-min washes with 1X PBS, sections were mounted to slides (Fisher Superfrost Plus) with the ProLong Gold Antifade mounting medium (Invitrogen). Images of antibody stained sections were acquired with an Olympus BX-51 fluorescence microscope using wide-field mode.

QUANTIFICATION AND STATISTICAL ANALYSIS

All statistical tests were conducted in Prism 7 analytical software (GraphPad). All datasets were first tested for normality using Shapiro-Wilk normality test as recommended [56]. Dataset normality was calculated without performing any transform (e.g., log10, or z-score) on the dataset. Outliers were removed using ROUTs outlier test in Prism 7 with Q = 1%. Statistical tests including ANOVA, Pearson correlations, t tests, and their non-parametric equivalents were performed in a similar matter to previous research. Post hoc analysis to adjust for multiple comparisons was used in accordance with Prism 7 statistical guide. Alpha was set to 0.05 for all analyses and was always calculated in a two-tail manner. Graphical representations of data were created using Graphpad Prism 7 and MATLAB.

Behavioral Task Performance

Animals' total errors on the familiar and altered task were divided by 15 laps to show the average number of errors per lap and analyzed using repeated-measures two-way ANOVA (Sidak post hoc) for performance within a group across days and two-way ANOVA (Tukey post hoc) for comparing between groups. For the difference between map errors and procedural errors the total number of each type of error was analyzed rather than error per lap. A repeated-measures two-way ANOVA (Tukey post hoc) was used to analyze within each error type and a two-way ANOVA (Sidak post hoc) was used to compare both types of errors.

Sleep State Analysis

Sleep/waking states were scored manually using CA1 LFP and EMG recordings in the same manner as Emrick et al. [57]. As the present study focuses on hippocampal learning and sleep, and previous work from our lab showed that the cortex and the hippocampus can be in two different sleep states simultaneously [57], CA1 LFP recordings were used instead of cortical EEG for sleep scoring and spindle identification. LFP and EMG recordings were down-sampled to 1000 Hz Epochs (10 s) were assigned a state of active waking, slow-wave sleep (SWS), Intermediate Sleep (which is a non-REM sleep state with high spindle power and occurrence, equivalent to

Stage 2 non-REM sleep in humans), or REM sleep using a sleep scoring program developed in our lab [58]. The percentage of time spent in sleep across days within each group and between groups was analyzed using a two-way ANOVA (Sidak post hoc).

Power Spectral Band Analysis

Down-sampled raw LFP from intervals of each scored state were entered into Neuroexplorer 5 software (Nex Technologies, Madison, AL). LFP data underwent a Fast-Fourier transform (FFT) using a window with a Hann taper. Change from baseline was identified using raw spectral power normalized to baseline across bands and expressed as a percent change from baseline by: ((day 1 – Baseline/ Baseline) * 100%). The percent change from baseline to day 1 sleep in the full power spectra and the specific bands was analyzed using a two-way ANOVA (Sidak post hoc). The percent change from baseline to day 1 in REM sleep theta power was analyzed further in Figure 6 via Mann-Whitney test.

Sleep Spindle and Ripple Identification

Sleep spindles were identified automatically from the entire sleep record. Automatic spindle identification was performed according to Eschenko et al., 2006 [34]. Briefly, the sigma frequency (10-15 Hz) was filtered in the CA1 LFP data down-sampled to 200 Hz, taking the root-means-square (RMS) over a 100 msec window, then smoothing it with a moving average. Spindles were counted from periods at least 0.3 s in length where the RMS exceeded three times the standard deviation of the RMS mean of all NREM sleep intervals. Reduction in NREM sleep spindle occurrence from baseline to 2 Hz stimulation was analyzed via paired t test in Figure 1. The percent change in spindle occurrence between baseline and day 1 was analyzed via Mann Whitney Test in Figure 6.

Ripples were automatically identified similar to the methodology described in Girardeau et al., 2009 [59] using a custom script written in MATLAB. Using the RMS of the 100-200 Hz bandpass filtered LFP, ripples were identified when the RMS crossed an upper threshold of five times the standard deviation of the average RMS for NREM and IS sleep. Ripple edges were detected when the RMS fell below a second threshold of two times the RMS standard deviation. Ripples were considered only in segments corresponding to NREM sleep states. Ripple occurrence and ripple length between groups and days was analyzed with a two-way ANOVA (Sidak post hoc) whereas percent change in ripple length and occurrence from baseline was analyzed via Mann Whitney Test.

Ripple-Spindle Coupling

Spindles and ripples were automatically identified (see previous section). Using custom MATLAB scripts, peri-event time histograms (PETHs) were generated using the start time of ripples as the event, and the start time of the spindles as the corresponding response. A range of 2500 msec prior to and following ripple onset was used, and bins were 50 msec in width. The number of spindle start times per bin was then divided by the total number of events (ripple start times) to convert to normalized probability. To test that this ripple-spindle coupling was non-random, shuffled ripple start time data (n = 15 per animal per day) was generated using a Monte Carlo method similar to Siapas 1998 [2] (we note this method of shuffle can be liberal). Shuffling was performed only during periods of NREM sleep to prevent an artificial reduction in the shuffled correlations. Spindle probability between ChR2- and ChR2+ rats, as well as either group versus shuffled data was analyzed via two-way ANOVA (Sidak post hoc).

Single Unit Isolation

Spike data were sorted into individual neurons using Offline Sorter x64 V3 (Plexon). For each tetrode recording of spikes, the data was manually sorted into single units using spike features of each of the four channels of the tetrode (e.g., principle component analysis or peak amplitude of each channel). LC call and CA1 pyramidal cell firing rate by state was analyzed using a repeated-measures two-way ANOVA with Sidak post hoc.

Place Cell Identification and Analysis

Following unit isolation, CA1 units were first separated into pyramidal cells and fast spiking interneurons based upon firing rate while the animal was running on the maze, as well as by spike width (pyramidal cells having a wider spike than fast-spiking interneurons). Interneuron data was then discarded from future analysis. Position tracking data from the rats running on the octagonal tract was separated into laps for the familiar and altered task. The track was then broken into 3 cm bins and linearized. Pyramidal cell spiking data was then used to generate raw rate maps and occupancy maps. Periods of less than 5 cm/s velocity were removed. Information content was calculated as in Skaggs et al., 1993 [60]. Cells with less than an information content of 0.15 were removed similar to Fuhs et al. [61] and all cells that were not active a minimum of five laps on a maze were also discarded. A Gaussian smoothing filter (SD = 4) was then applied to the firing rate data. Cells were determined to be place cells if their smoothed firing rate crossed threshold (1 Hz) for 3 or more consecutive 3 cm bins, in addition to meeting the above criteria. Place cell stability or lap to lap correlation (r), was computed per cell via a bin-by-bin Pearson's correlation between firing rate maps for all laps that the cell was active similar to [62]. Place cell average lap to lap correlation cumulative probability was analyzed using K-S test, and average day 2 place field lap to lap correlation were analyzed via Mann-Whitney test. Place field absolute shift and size were analyzed using a Kruskal Wallis (Dunn post hoc) and place field center of mass shift from original position was analyzed using a two-way ANOVA (Dunnett post hoc).